THE ESTIMATION OF NONLINEAR SITE EFFECT FROM THE SURFACE MOTION

Kyi Kyi Swe* **Supervisor: Toshiaki, YOKOI****
MEE10506

ABSTRACT

We have conducted a case study for recently proposed parameter of non-linear site response *DNLs*. The data are used the accelerograms of the 2011 off the Pacific coast of Tohoku earthquake and its aftershocks, mainly, recorded at three KiK-Net stations that have vertical arrays.

Besides *DNLs* PGA amplification is considered as a reference parameter. In FKSH14 and IBRH13, a significant de-amplification is observed in the range of PGA at the borehole bottom greater than 10 gals; also in the range of PGA at the ground surface greater than 100 gals, whereas in IBRH18, it is not observed with the only exception, i.e., the main shock. It is observed that *DNLs* increases with the PGA both at the ground surface and borehole bottom in the range as mentioned above for all three stations. *DNL* based on the horizontal to vertical spectral ratio of the surface record ($DNL_{S\text{-}H/V}$) well follows the behavior of that based on the spectral ratio of the surface records to those obtained at the borehole bottom (DNL_{SB}) and shows a possibility to use the former in place of the latter if only surface records are available. We may expect that these *DNLs* will be useful for the future strong motion study in Myanmar.

Keywords: Nonlinear site effect, Vertical array, DNLs, PGAs, PGA-amplification.

1. INTRODUCTION

In this study we cannot use any strong motion data obtained in Myanmar due to lack of a digital strong motion seismograph network. We use the data of the Off the Pacific Coast of Tohoku Earthquake on March 11/14:46, 2011 (Mw=9.0, Event 2 in Table 1), which occurred near the northeast coast of Honshu, Japan. The hypocenter depth of the earthquake is 20 km and is located in the subduction zone of plate boundary between the Pacific and North American plates. This earthquake generated strong ground motions over a wide region of Tohoku in Japan. We investigate the influences of nonlinear site responses on these strong motion data. The purpose of this study is to conduct a case study using real strong motion data for the recently proposed parameters that describe the non-linear response of soil layers *DNLs* (Noguchi and Sasatani 2008; 2010): to verify their capacity to characterize the non-linearity; to verify the applicability to the cases where only surface records are available.

2. DATA

We use the strong motion data obtained by the KIK-Net stations, NIED, Japan, at which they have both surface sensor and another at the bottom of a borehole that reaches to the basement composed of the hard rock. The vertical array data is available at KiK-Net stations. These vertical arrays provided us the possibility to verify the DNL approach. In this study we mainly use the main shock's and aftershock's records of this earthquake and a few other earthquakes additionally.

---

*The author works for Department of Meteorology and Hydrology, Ministry of Transport, Myanmar.
**International Institute of Seismology and Earthquake Engineering, Building Research Institute, Tsukuba, Japan.

Table 1. Strong motion records used in the analysis (After KIK-Net web site)

Event ID	Date_&_Time	Latitude	Longitude	Magnitude	Depth
1	2010/09/30/01:23:47	37.28	140.01	4.6	7
2	2011/03/11/14:46:55	38.10	142.86	9.0	24
3	2011/03/11/15:15:00	36.11	141.27	7.7	43
4	2011/03/12/22:15:00	37.20	141.43	6.2	40
5	2011/03/14/10:02:47	36.46	141.12	6.2	32
6	2011/03/16/12:52:15	35.84	140.91	6.1	10
7	2011/03/19/18:56:20	36.78	140.57	6.1	5
8	2011/03/23/07:12:32	37.08	140.79	6.0	8
9	2011/03/23/07:36:00	37.06	140.77	5.8	7
10	2011/04/11/17:16:00	36.90	140.70	7.1	10
11	2011/04/12/14:07:48	37.00	140.70	6.3	10
12	2011/04/12/14:26:46	37.00	140.70	4.9	20
13	2011/04/23/00:25:00	37.20	141.30	5.6	20
14	2011/04/24/19:09:00	37.10	140.70	4.4	20
15	2011/05/10/08:38:38	36.70	140.70	4.4	10

We select the records obtained at IBRH13, IBRH18 and FKSH14 stations. The events parameters are listed in Table 1. These records are selected using criteria: the focal depth less than 40Km and epicentral distance shorter than 100Km, mostly. The geological condition and the location of three stations are; IBRH13 has weathering rock at the shallowest part and is located in the northern part of Ibaraki Prefecture. IBRH18 has shallow sandy gravel layer and located in the middle Ibaraki Prefecture and FKSH14 has sand layer and Located in the southern part of Fukushima Prefecture.

3. METHOD OF STUDY

3.1. Degree of Nonlinear Site Response

Noguchi and Sasatani (2010) have proposed new indicators *DNL (Degree of non-linearity)* for a non-linear behavior of shallow soil layers as follows. The response of a shallow layer is directly given by the spectral ratio of a horizontal component of the surface record to that obtained at the bottom of a borehole. At a low strain level, i.e., weak ground shaking, this gives a linear amplification (hereafter denoted as a function of the frequency $R^{SB}_{weak}(f)$). At a strong ground shaking, the amplification will be changed due to a non-linear behavior of soils and becomes different from the original linear one (hereafter denoted as a function of the frequency $R^{SB}_{strong}(f)$). They define an indicator of a non-linear behavior DNL_{SB} using the ratio of these spectral ratios of surface to borehole records. They also define another indicator $DNL_{S\text{-}H/V}$ using the spectral ratio of a horizontal component to a vertical one of surface records based on the observation reported by Wen et al. (2006): this spectral ratio at a ground shaking, strong enough for non-linear response $R^{S-H/V}_{strong}(f)$, differs from that at a weak ground shaking $R^{S-H/V}_{weak}(f)$.

DNL is defined as follows

$$DNL = \sum \left| \log \frac{R_{strong}(f)}{R_{weak}(f)} \right| \Delta f, \qquad (2)$$

where the summation is taken over the frequency from 0.5 Hz to 20 Hz (Figure 6 right). This denotes the area between the two spectral ratio curves in full logarithmic graph. For DNL_{SB}, $R_{weak}(f)$ and $R_{strong}(f)$ are replaced with $R^{SB}_{weak}(f)$ and $R^{SB}_{strong}(f)$, respectively, whereas for $DNL_{S\text{-}H/V}$ with $R^{S-H/V}_{weak}(f)$ and $R^{S-H/V}_{strong}(f)$, respectively. DNL_{SB} requires both of surface and borehole records, whereas $DNL_{S\text{-}H/V}$ requires only surface records of three components.

4. RESULTS OF ANALYSIS

4.1 De-Amplification Effect

We analyzed the relation of PGA (Peak Ground Acceleration) amplification at the ground surface and at the bottom of a borehole in order to investigate the influence of nonlinear site responses on strong motion records (Figure 1). Here, PGA amplification means the ratio of PGA at the surface to that at the bottom of a borehole; PGA is calculated as the vector sum of the maximum absolute value of North-South and that of East-West components.

The value of PGA amplification is limited to below 12 gals for all of these three stations. A de-amplification is observed clearly at FKSH14 (Figure 11 a) and b)) and IBRH13 (Figure 11 c) and d)): the bigger PGA both at the ground surface and the borehole bottom correspond to the lower PGA amplification, therefore to the stronger non-linearity. In these two stations a significant de-amplification of the strong motion is observed in the range of PGA at a borehole bottom greater than 10 gals; also in the range of PGA at the ground surface greater than 100 gals.

On the other hand, in IBRH18 a de-amplification effect is not observed as clearly as in others (Figure 1 e) and f)). Only the mark of the maximum PGA that is of the main shock (Event 2) shows the graph slightly decaying, but others' PGA amplifications are aligned almost constant. This seems to imply a linear response of IBRH18 except for the Event 2. However, the limitation of PGA amplification implies non-linearity. It's better to verify another parameter of non-linearity, *DNLs*.

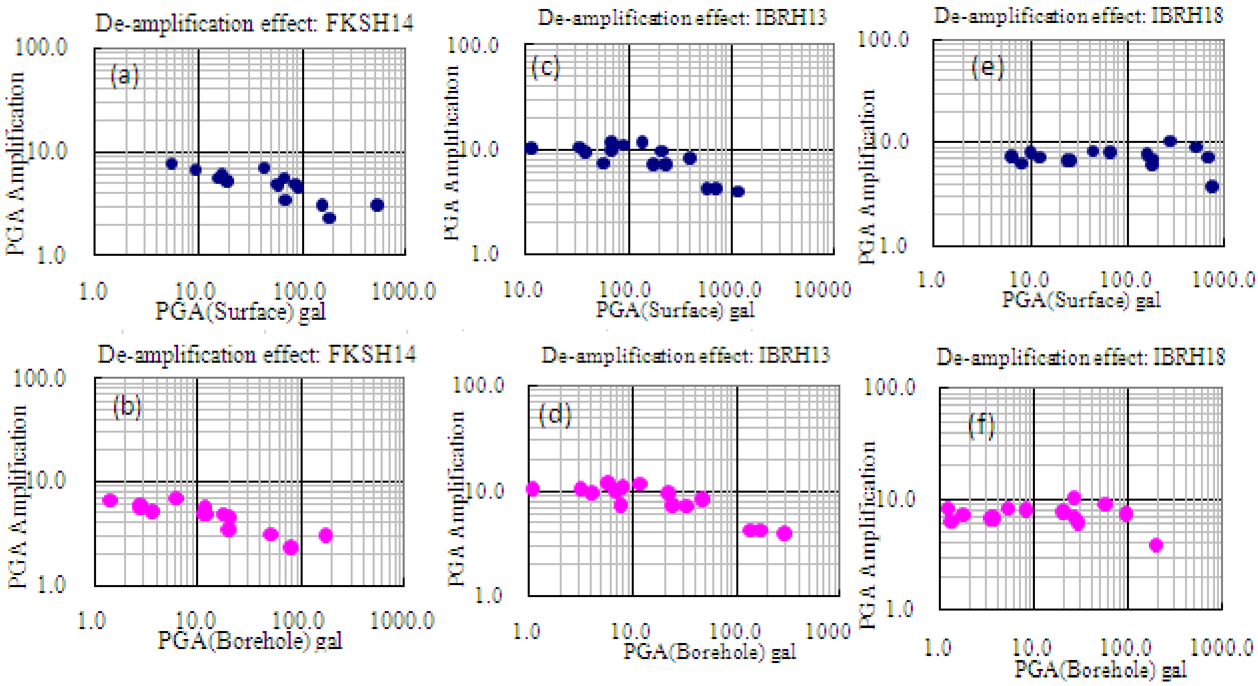

Figure 1. Relations of PGA amplification factor to PGA: a) FKSH14, to PGA at the surface, b) FKSH14, to PGA at the borehole, c) IBRH13, to PGA at the surface, d) IBRH13, to PGA at the borehole, e) IBRH18, to PGA at the surface, f) IBRH18, to PGA at the borehole.

4.2 Change of Spectral Ratio Curve due to Non-Linearity

We calculated (1) the spectral ratio of surface records to the corresponding one recorded at the borehole bottom (surface/borehole or S/B), (2) the ratio of a horizontal component at the surface to a vertical component at the surface (S-H/V) and (3) the ratio of these spectral ratios of a strong ground motion to that of a weak ground motion in order to observe the degree of nonlinear behavior, or DNLs.

Examples are shown in Figure 2. In Figure 2, the records at FKSH14 due to Event 2 (Mw=9.0) and Event 14 (M=4.4) are compared as examples to explain the procedure of this analysis. In panels a) and d) the spectral ratios (surface/borehole) of Event 2 and 14 are shown with solid curves, respectively, while the dotted curve shows that of Event 15 (M=4.4), i.e., the reference event in this study.

For a linear response case, panel d) shows the solid curve almost identical to the dotted curve. DNL_{SB} of the panel d) is 2.107. Panel e) shows the spectral ratio (S-H/V) and its quite similar tendency as panel d) with $DNL_{S\text{-}H/V}$ 2.862. The solid curve of panel f) shows the ratio of the spectral ratio (surface/borehole) of Event 14 to that of Event 15 shown by the solid and dotted curves in panel d), respectively. Due to the similarity of these ones, the solid curve in the panel f) deviates around 1.0. A similar procedure is taken to draw the dotted curve in panel f) from the solid and dotted curves in panel e).

For a non-linear response case, panel a) shows a significant reduction of amplification and the peak shift toward lower frequency for the solid curve (Event 2) in comparison with the dotted curve (Event 15). DNL_{SB} of panel a) is calculated to be 8.179. Panel b) shows the spectral ratio (S-H/V), which shows a quite similar tendency as that of panel a). $DNL_{S\text{-}H/V}$ of panel b) is calculated to be 8.052. In panels a) and b) the difference between the solid and dotted curves appear in the frequency range from 1 Hz to 3Hz and 5Hz to 15Hz.   This is reflected to panel c). The solid curve in panel c) shows the ratio of the spectral ratio (surface/borehole) of Event 2 to that of Event 15 shown by the solid and dotted curves in panel a), respectively. Due to the strong non-linearity, the solid curve in the panel c) has a systematic decay from 1.0 in the above mentioned frequency range. A similar procedure is taken to draw the dotted curves in panel c) from the solid and dotted curves in the panel b).

The behavior of the dotted curves in panels c) and f) is quite similar to that of the corresponding solid curves and shows a possibility to use the spectral ratio S-H/V in place of the spectral ratio (surface/borehole).The same procedure as these examples is applied for all other events and for all stations. The result will be described in the following.

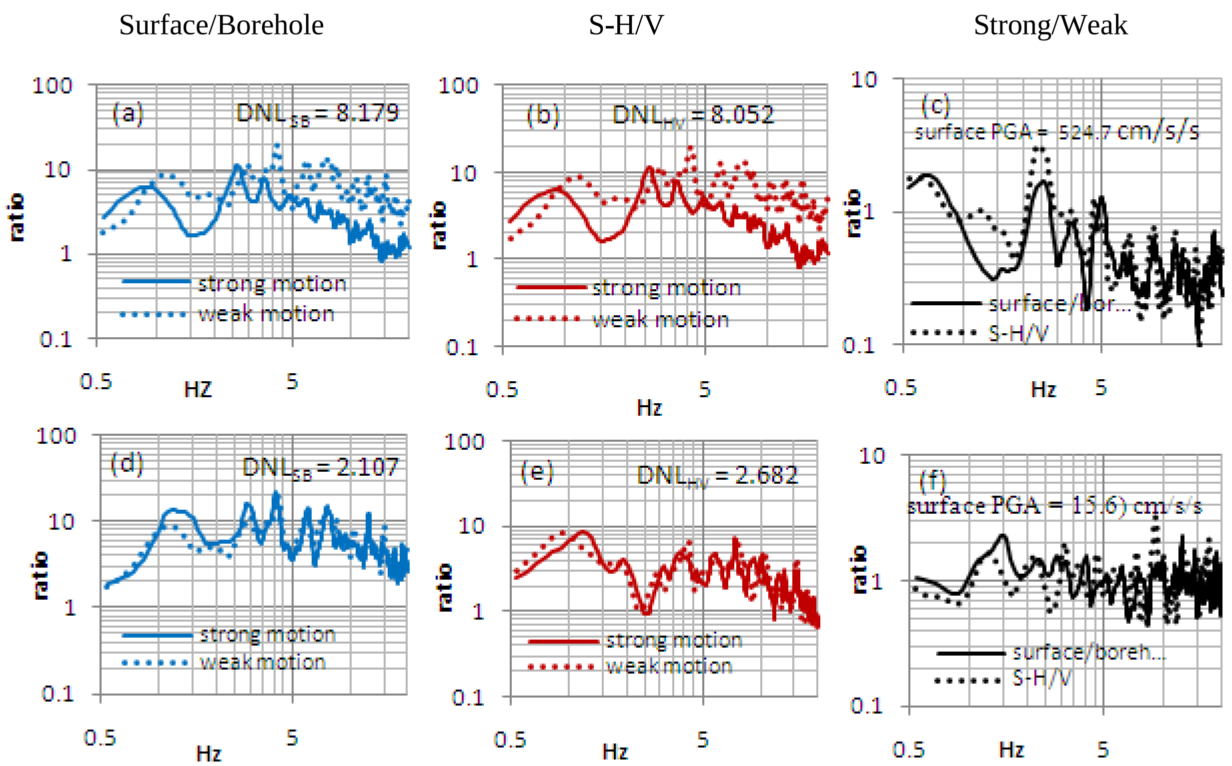

Figure 2. Example of change of spectral ratios at FKSH14 due to Event 2: a) Spectral ratio (surface/borehole), b) Spectral ratio (S-H/V), c) Ratio of spectral ratios (strong/weak). Those due to Event 14: d) Spectral ratio (surface/borehole), e) Spectral ratio (S-H/V), f) Ratio of spectral ratios (strong/weak).

4.3 Degree of Non-Linearity: DNL_{SB} and $DNL_{S\text{-}H/V}$

We compared the relation of *DNL*s to PGA at the ground surface and at the borehole bottom in order to confirm the influence of nonlinear site responses on the strong motion (Figure 3).

It is observed that DNL_{SB} increases with the PGA both at the ground surface and the borehole bottom in the range PGA (surface) bigger than 100 gals and PGA (borehole) bigger than 10 gals. The behaviors of FKSH14, IBRH13 and IBRH18 look similar. Below this threshold, any clear trend cannot be found. It is also observed that $DNL_{S\text{-}H/V}$ follows the change of DNL_{SB}. Above the threshold mentioned, $DNL_{S\text{-}H/V}$ takes close value of DNL_{SB}, whereas below it $DNL_{S\text{-}H/V}$ tends to differ from DNL_{SB}. This may be due to a fluctuation of observed spectra or other disturbance.

Figure 3 shows a clear relation of DNLs to PGAs and possibility to use $DNL_{S\text{-}H/V}$ in place of DNL_{SB} above the threshold value of PGA (surface) bigger than 100 gals.

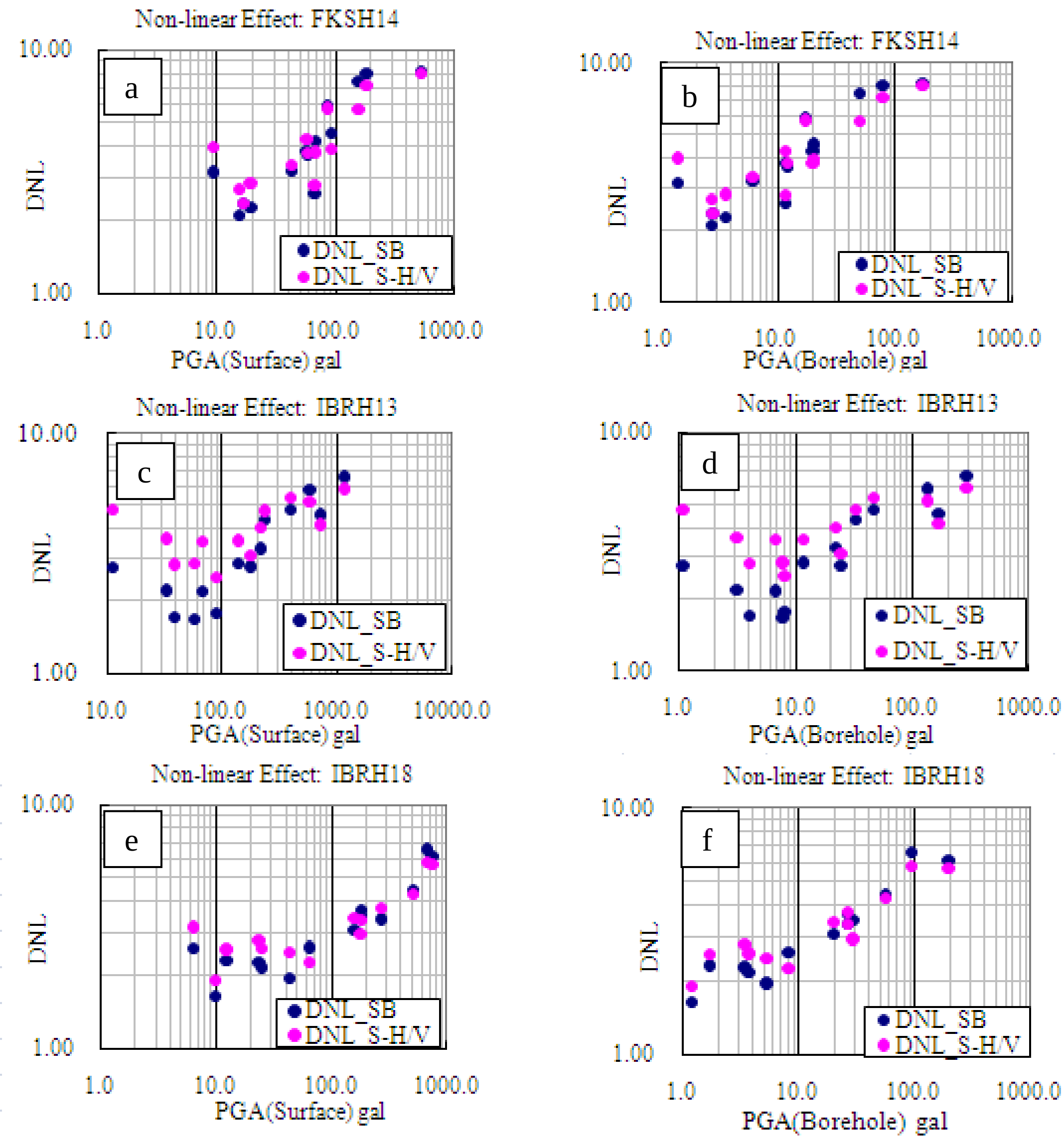

Figure 3. Relation of *DNLs* to PGA: a) FKSH14, to PGA at the surface, b) FKSH14, to PGA at the borehole, c) IBRH13, to PGA at the surface, d) IBRH13, to PGA at the borehole, e) IBRH18, to PGA at the surface, f) IBRH18, to PGA at the borehole.

5. DISCUSSION AND CONCLUSIONS

We have conducted a case study for *DNLs* recently proposed by Noguchi and Sasatani (2010). The data are used the accelerograms of the 2011 off the Pacific coast of Tohoku earthquake (Mw=9.0) and its aftershocks, mainly, recorded at three KiK-Net stations in Fukushima and Ibaraki Prefectures: FKSH14 sandy site; IBRH13 weathering rock site; and IBRH18 sand and gravel site. In FKSH14 and IBRH13, smaller PGA amplification corresponds to bigger PGA at the ground surface and also at the borehole bottom. Namely, a significant de-amplification of the strong motion is observed in the range of PGA at borehole bottom greater than 10 gals; also in the range of PGA at the ground surface greater than 100 gals, whereas in IBRH18 de-amplification is not observed with the only exception, i.e., the main shock (Event 2).

It is observed that *DNLs* increases with the PGA both at the ground surface and borehole bottom in the range of PGA at the ground surface bigger than 100 gals and PGA at the borehole bottom bigger than 10 gals. The behaviors of FKSH14, IBRH13 and IBRH18 look similar. Below this threshold, any clear trend cannot be found.

For the above two, $DNL_{S\text{-}H/V}$ well follows DNL_{SB}. The curve $R^{S-H/v}_{strong}(f)/R^{S-H/V}_{weak}(f)$ fits well to the curve $R^{SB}_{strong}(f)/R^{SB}_{weak}(f)$. This shows a possibility to use the former in place of the latter when only surface records are available.

All these results of analysis support Noguchi and Sasatani (2010). We may expect that *DNLs* and methods of Noguchi and Sasatani (2010) will be useful for the future strong motion study in Myanmar.

Nonlinear site effect is one of the key issues to investigate past ground shakings and to estimate future ones. It is a common sense that a detailed study of underground structures is necessary to improve the understanding of nonlinear site effects which is indispensable for the earthquake hazard and risk assessment and further earthquake disaster mitigation. The current strong motion observation in Myanmar, however, has accelerographs on the ground surface only. A way to estimate nonlinear behaviors of shallow soil layers using only records obtained at the ground surface is desired. In this study, we analyzed nonlinear site effects of a strong ground motion obtained by the KiK-net vertical array, by checking the relation between the site responses and the strength of a ground motion. A trend that is not very clear but visible is observed in the plots of *DNLs* against PGA amplification and those against PGA at the surface. These may allow us to estimate, roughly, PGA at the engineering bedrock from the data obtained at the ground surface.

Nowadays, Myanmar is planning to improve new seismic stations. So, I hope that seismic data of Myanmar can be used to investigate nonlinear site effects of a strong ground motion, after installation of new seismic stations.

AKNOWLEDGEMENT

I am sincerely thankful to the National Research Institute for Earth Science and Disaster Prevention (NEID), Japan for providing the waveform data for my study and to Dr. Toshihide Kashima (IISEE, BRI) for the software View Wave.

REFERENCES

Noguchi, S. and Sasatani, T., 2008, Proc. of 14th WCEE.
Noguchi, S., and Sasatani, T., 2010, Proc. of 13th Japan Earthquake Engineering Symposium, PS3.
Wen, K., et al. (2006), Terrestrial Atmospheric and Ocean Sciences, 17, 533-546.
Kashima, T., 2009, View Wave software (version 1.56),
http://iisee.kenken.go.jp/staff/kashima/software_e.html
KIK-NET web site, http://www.kik.bosai.go.jp/kik/index_en.shtml